

Three components of the superconducting response in high-resistance metastable states of the alloy Cd–Sb

V. F. Gantmakher, V. N. Zverev, V. M. Teplinskii, and O. I. Barkalov

Institute of Solid State Physics, Russian Academy of Sciences, 142432 Chernogolovka, Moscow Province
(Submitted 11 November 1993)

Zh. Eksp. Teor. Fiz. **105**, 423–438 (February 1994)

The evolution of the superconducting transition during the transformation of the metastable alloy Cd–Sb into the insulator state is investigated. It is shown, on the basis of measurements of the temperature and magnetic-field dependence of the electric resistance and the dynamic magnetic susceptibility, that this system can be described as a finely dispersed medium with irregularities whose size exceeds the coherence length. It is established that the superconducting response in Cd–Sb near the metal-insulator transition contains three components: a decrease in the resistance due to the presence of superconducting granules and another due to Josephson currents and an increase of the resistance due to freezing out of single-particle tunneling current between superconducting granules.

1. INTRODUCTION

The superconducting (s) response in three-dimensional (3D) materials with high resistivity is substantially different from the standard superconducting response. Many diverse manifestations of such differences are known. The transition may become incomplete with the resistance R assuming a constant value R as the temperature T decreases¹ or the transition can become quasireentrant, i.e., R increases again as T decreases.^{2,3} It can even be characterized by sharply accelerated growth of R at temperatures $T < T_c$ —the inverse superconducting response.^{4,5} Giant negative magnetoresistance can be observed near the transition,^{5,6} and increasing the electric current can stimulate either a re-entrant transition, i.e., increase R at $T < T_c$,⁷ or superconductivity.⁸

Most of these phenomena are usually attributed to spatial gradients of the material. Thus there naturally arises the problem of the superconducting response in a spatially nonuniform medium.

A nonuniform material is most often modeled by metallic (M) granules in an insulating (I) matrix.^{9–11} It is well known that for the normal state the scaling hypothesis^{12,13} describing the metal-insulator transition does not make any qualitative distinctions between granular material and a semiconductor containing statistically distributed impurities,^{11,14} though the characteristic lengths in these two cases can be completely different. Granules play the role of impurity centers, and tunneling between them is equivalent to hops from one center to another.^{15,16}

It is not clear whether a similar universality exists for superconducting properties. It is to the granular structure of the material that the inverse superconducting response and the giant negative magnetoresistance are attributed. The resistance increases with decreasing temperature because the superconducting gap in the system results in an exponential decrease of the single-particle tunneling current through the interlayers between the superconducting granules.¹⁷ A magnetic field obliterates the gap and for this

reason the resistance decreases. However, the question of how the superconducting response will change as the sizes of the granules gradually decrease and the material becomes quasiuniform, so that disorder is realized at the atomic level and granules and clusters are formed from elements of atomic size according to the laws of statistics, has not been solved either theoretically or experimentally.

It is from this point of view that the experimental data discussed in this paper on the superconducting response of metastable high-resistance states of the alloy Cd–Sb must be considered. This paper is organized as follows.

The next section is devoted to methodological questions. A method for obtaining the sequence of states of the material, together with a set of resistivities over several orders of magnitude, is described. Starting with the quenched metastable high-pressure metal phase, these states were obtained from one another by proportioned annealing; in the process, the metal properties of the material were gradually replaced by insulator properties.

A description formulated for the metal-insulator transition in this material on the basis of measurements of the transport properties of the normal state is contained in Refs. 18 and 19. In the present paper the evolution of the superconducting response of the system is mainly discussed. The experimental data are assembled in Sec. 3. They contain the results of measuring the temperature dependence of the resistance (Sec. 3.1) and dynamic susceptibility (Sec. 3.2), as well as the effect of magnetic and electric fields on them, for a sequence of 20 states of the alloy Cd₄₇Sb₅₃. These results can be summarized as follows: Below the transition point T_c the dc superconducting response in the metastable alloy Cd₄₇Sb₅₃ near the localization threshold has three components:

1. A London (L) component, which decreases the resistance R of the material, though it does not reduce R to zero. This superconducting current is destroyed, as usual, by the temperature-dependent field H_{c2} .

2. A Josephson (J) component, which also decreases the resistance R and is destroyed by a much weaker, temperature-independent, field $H_J \ll H_{c2}$.

3. An incoherent (U) component with a negative sign. This component is manifested as a sharp increase of the resistance at $T < T_c$ in the absence of a magnetic field and as giant negative magnetoresistance on the scale of the fields $H_{c2}(T)$. This component, like the London component, is destroyed by the field $H_{c2}(T)$.

The appearance of all three components has a rational explanation within the model of a granular metal. This explanation is formulated qualitatively in Sec. 3.1 immediately after the exposition of the results. The simplest quantitative model, constructed in the mean-field approximation, is presented separately in Sec. 4.1. According to this model a three-component superconducting response with the observed ratio of the components is indeed possible in a granular metal.

An explanation of the characteristic lengths in the experiment is constructed similarly. A presentation of the results following directly from measurements of the dynamic susceptibility concludes Sec. 3.2, and a general analysis is given in Sec. 4.2, the second part of the Discussion section. Analysis shows that the size of characteristic structural nonuniformities exceeds the coherence length ξ . This justifies the application of the granular-metal model.

In the final section, comparing the superconducting response to the temperature dependence $R(T)$ in the normal state, we return to the questions concerning the structural nonuniformities and their nature and the possible scenarios of evolution of the superconducting response in quasiuniform high-resistance materials.

2. EXPERIMENT

The Cd-Sb system at high pressures and temperatures has a metal phase, which can be quenched and maintained indefinitely in the metastable state at liquid-nitrogen temperature. On heating, this metal phase gradually transforms into an x-ray-amorphous insulator state, and in the case of the composition $Cd_{47}Sb_{53}$ this state does not have any crystalline inclusions.^{20,21} This state is in turn also metastable, but it passes into an equilibrium crystalline state at temperatures above room temperature.

The systems Zn-Sb and Ga-Sb, whose transport properties we investigated previously,^{6,22} also have a similar property. In the process of amorphization the specific volume of all these systems increases.^{20,23} This promotes the formation of specific fractal structures during the transformation process.²⁴ But, in Zn-Sb and Ga-Sb the specific volume increases by approximately 25%, whereas in Cd-Sb it increases by only 12.5%.^{21,25,26} For this reason, there are grounds for expecting that the intermediate states in such materials will have different structures.

Specimens with approximate dimensions of $1 \times 1.5 \times 8$ mm³ made from the alloy $Cd_{47}Sb_{53}$ were held for 1.5 h in a high-pressure chamber²⁰ at a pressure of 65 kbar and temperature of 250 °C. Then the temperature was lowered to the temperature of liquid nitrogen at an average rate of about 20 °C/sec, after which the pressure was removed. According to the Debye powder pattern, the samples obtained were polycrystalline and had a simple hexagonal structure.²⁰

Two samples were employed simultaneously in the experiment. One was clamped in a holder by two pairs of 0.5 mm in diameter gold wires with pointed ends, which simultaneously served as electric contacts. The second sample was placed inside one of two identical coils situated on the same holder and used for measuring the dynamical susceptibility. The samples were mounted in the holder at the temperature of liquid nitrogen. Next, the holder with the samples was placed in a hermetically sealed chamber, connected with a bottle of He³. The temperature in the chamber could be varied from 0.5 to 300 K. The chamber was placed in a cryostat with a superconducting solenoid. At temperatures below 1.5 K the samples were in liquid He³, while above 1.5 K the samples were in a heat-exchange gas. The temperature was recorded from indications of a resistance thermometer. The thermometer was graduated at low temperatures on the basis of the He³ vapor pressure.

We were interested in the collection of intermediate states between the initial metastable metal phase and the disordered insulator phase. The transition from one intermediate state into another was made by heating the sample up to room temperature and holding the sample at this temperature for some time, monitoring the temperature by continuously measuring the resistance, which gradually increased. The holding period was interrupted so that the resistance of the sample at 6 K could increase by a factor of 1.5–2. The holding time depended on the transformation stage; for the high-resistance insulator states it reached several hours. At temperatures below room temperature the state of the sample was not affected by any regime of temperature variation, so that the low-temperature measurements could be performed indefinitely. A total of 20 states, in which the resistance at $T = 6$ K varied over six orders of magnitude, were investigated. In the initial state the sample had a resistivity of order $170 \mu\Omega \cdot \text{cm}$.

The resistance and magnetoresistance as well as the current-voltage characteristics were measured on a sample with clamping contacts. The measurements were performed by the four-contact method, using mainly a 36-Hz ac current. The values of the resistance obtained in dc control experiments were the same as for ac current.

The contactless measurements of the dynamic susceptibility were performed by the bridge method at a frequency of $3 \cdot 10^4$ Hz. The signal was normalized to the magnitude of the response obtained when the alternating magnetic flux was completely expelled from the volume of the sample. The normalization response was determined from the superconducting transition measured in a lead sample having the same dimensions, at low frequencies when the normal skin effect can be neglected. The measurements of the dynamic susceptibility could be performed with different amplitudes of the ac magnetic field H_{ac} in an interval approximately from 5 to 10^{-4} Oe. This made it possible to separate the contributions of the Meissner effect on massive superconducting regions and currents flowing through the superconducting contacts along closed circuits from superconducting granules and screening the normal regions.

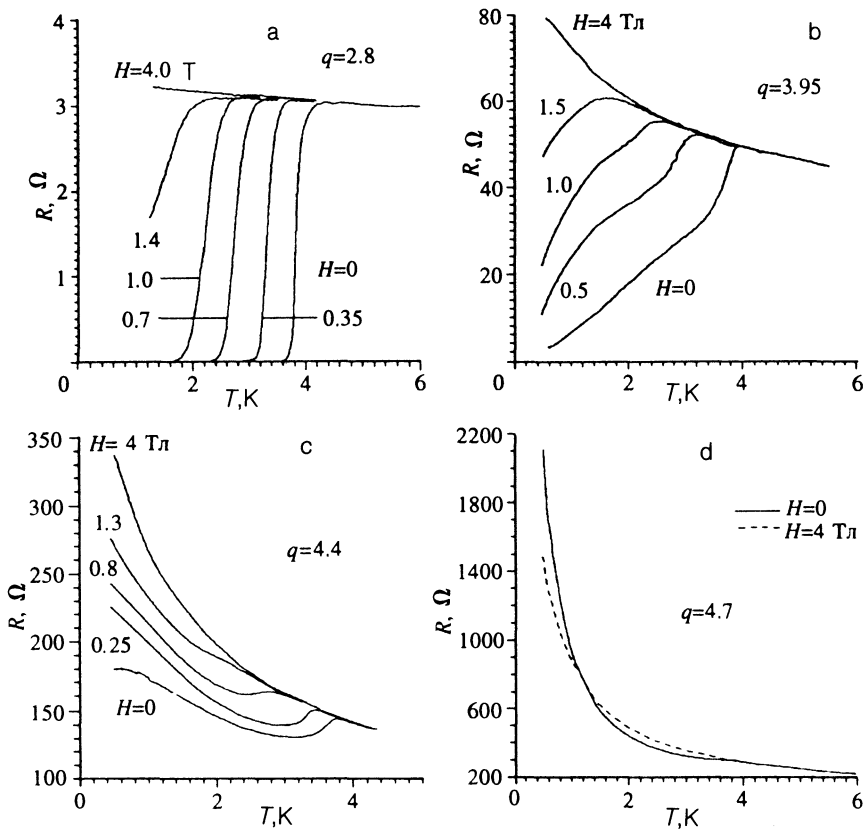


FIG. 1. Temperature dependence of the resistance of a sample in different states q as a function of the magnetic field.

The holder with the samples could be turned with respect to the direction of the constant magnetic field. However, neither the angle between the field and measuring current nor the angle between the field and the coil axis was observed to have any effect on the measured functions. For this reason, in describing the results we do not indicate the direction of the magnetic field.

3. RESULTS

We characterize the instantaneous state of the sample by the parameter q determined in terms of the resistance of the sample at $T=6$ K:

$$q = \lg(R/R_{in})_{T=6 \text{ K}}, \quad (1)$$

where R_{in} is the resistance in the initial state, for which $q=0$. According to measurements of the normal-state conductivity σ the metal-insulator transition occurs at $q \approx 4$.¹⁸ This result was obtained by extrapolating to $T=0$ the temperature dependence in the interval 4–20 K, i.e., above the superconducting transition. It has now been reproduced in three series of measurements.

3.1. Resistive superconducting response

A set of curves of the superconducting transition in zero magnetic field was already presented in Refs. 6 and 27 for different states of the alloy Cd-Sb, i.e., for different values of q . For this reason we confine ourselves here to demonstrating how a magnetic field affects these curves. Figure 1 displays four series of curves $R(H, T)$ in different states and in different magnetic fields from $H=0$ up to the field $H=4T > H_c$, which certainly completely destroys su-

perconductivity. The first series of curves (Fig. 1a, $q=2.8$) has a quite standard form, if one ignores the fact that the limiting curve $R(T)|_{H>H_c}$, to which the transition curves shifting with the field toward lower temperatures converge, has a negative derivative $\partial R/\partial T$.

The further evolution of the superconducting transition with increasing q is shown in Figs. 1b–1d. The matter is not only a gradual increase of the slope of the limiting curve $R(T)|_{H>H_c}$. In the limiting state $q \approx 4$ the curves $R(H, T)$ apparently still drop to zero at $H=0$ and at finite subcritical values of H (Fig. 1b). Increasing q up to 4.4 makes the limiting value $R(H, 0)$ finite at $H=0$, while in a field $H \neq 0$ the resistance with increases with decreasing T (Fig. 1c). Finally, for even larger values of q the resistance R is observed to increase even in a zero field, and the increase in R is so strong that at low temperatures we already have $R(0, T) > R(H_c, T)$; see Fig. 1d. It is the intersection of the curves $R(T)$ at low temperatures for $H=0$ and for $H > H_c$ that is most significant and requires further analysis.

On the curves in Fig. 1a the temperature dependence of the second critical field $H_{c2}(T)$ is determined naturally from the shift of the superconducting transition as a function of the magnetic field. Assuming that the breaks in the curves $R(H=\text{const}, T)$ determine the field H_{c2} for large values of q also, a curve $H_{c2}(T)$ can be obtained in each state; some of these curves are displayed in Fig. 2. Increases in q and in H both lead to smoothing of the break, so that the accuracy with which H_{c2} is determined decreases. It can be asserted, however, that right up to $q \approx 5$ the field H_{c2} so determined, as also the temperature T_c ,^{6,27}

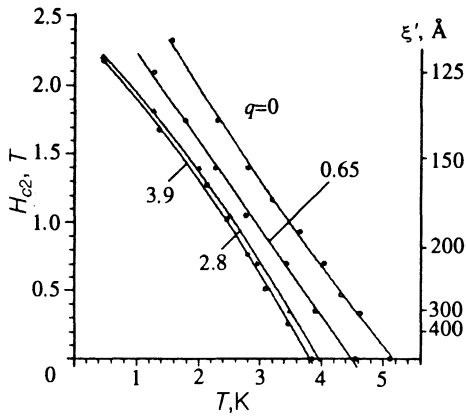


FIG. 2. Temperature dependence of the second critical field H_{c2} in different states of the sample. See Sec. 4.2 for a discussion of the right-hand scale.

is virtually independent of q . The derivative $\partial H_{c2}/\partial T$ remains practically unchanged at $T=T_c$:

$$\partial H_{c2}/\partial T = -0.6(T/K). \quad (2)$$

The fact that T_c and H_{c2} do not significantly depend on q means that even in each specific case we cannot expect strong dispersion of these quantities through the sample.

In order to analyze the structure of the superconducting response it is more convenient to use the field dependence $R(H, T)$ for different values of T . Figure 3 gives a collection of such curves in the state with $q=4.7$, which is located on the insulator side of the transition. This is a state that appeared in Fig. 1d. But Fig. 1d gives a general idea of the scale of the effect as compared to the temperature variation of R , and now we can study the effect in detail for different fixed temperatures. All curves in Fig. 3 are normalized to the resistance in the field $H=4T$. The dashed line is the magnetoresistance above T_c . It is very low: As the field decreases from $4T$ to 0, the resistance

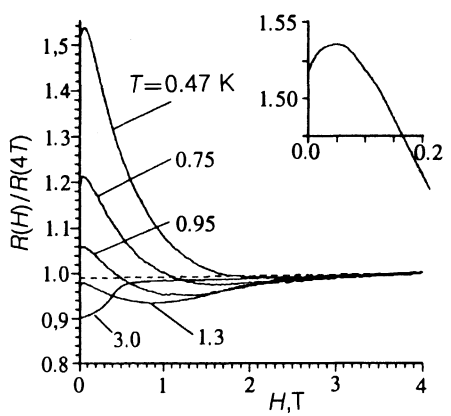


FIG. 3. Magnetic field dependence of the resistance at different temperatures for the state $q=4.7$. The dashed line indicates the dependence at $T=4$ K. Each curve is normalized to the resistance at the given temperature in the field $H=4$ T. Inset: The part of the curve at $T=0.47$ K on an enlarged scale.

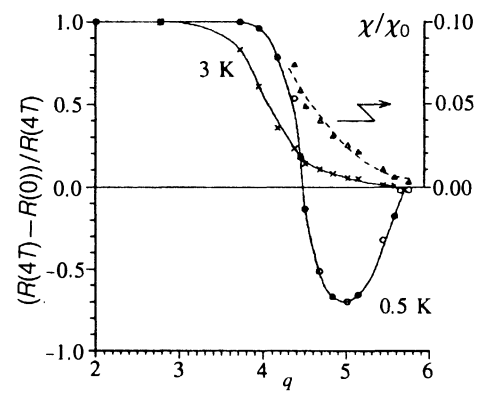


FIG. 4. Relative superconducting response at two temperatures (3 K and 0.5 K) and dynamic susceptibility as a function of the parameter q . The susceptibility is normalized to the signal corresponding to complete expulsion of the magnetic flux from the volume of the sample; the change occurring in the resistance when a field switched on is normalized to the value of the resistance in the field.

decreases continuously by less than 2%. This dashed line can be taken as the initial zero line, from which the superconducting response should be measured.

The other curves in Fig. 3 clearly demonstrate the existence of the three components of the superconducting response mentioned in the introduction. The natural decrease in resistance with decreasing field (L component) near T_c at first behaves normally, shifting in the direction of high fields with decreasing temperature. Then it is replaced by an increase in the resistance (U component) at low temperatures, leading to giant (nearly a factor of 2) negative magnetoresistance. Finally, in weak fields at low temperatures it is obvious that the field destroys another component (J) of the superconducting response, having the same sign as the L component (see also the inset in Fig. 3).

All doubts as to whether a component of the superconducting response and not some independent superposed effect, for example, hopping magnetoconduction, is responsible for the giant negative magnetoresistance are removed with further transformation of the state of the sample, pushing the sample deeper into the insulator region. The U component, which appeared near the metal-insulator transition at $q \approx 3$, vanishes at $q \approx 5$ together with all other manifestations of superconductivity (see Fig. 4).

The names given to the three components of the superconducting response are not, of course, accidental. A clear physical picture emerges from everything said above. Consider a granular superconductor. If the metal granules are separated by quite wide insulating gaps, then in the superconducting state all granules are completely independent and, as a result of the partial shunting of the low-resistance matrix by superconducting inclusions, the superconducting response contains only the L component. Josephson junctions between separate granules lead to an additional decrease of the resistance; the Josephson superconducting currents are, however, destroyed by a comparatively weak magnetic field (J component). If all contacts

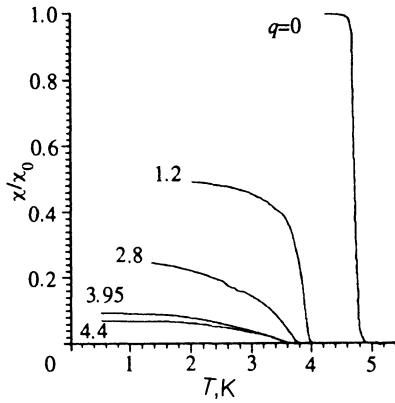


FIG. 5. Temperature dependence of the dynamic susceptibility for different values of q . The functions are normalized to the signal corresponding to complete screening of the volume of the sample.

are Josephson junctions, then the superconducting transition can split in two transitions: intragranular transition at T_{c0} followed by establishment of a coherent state in all granules with $T_c < T_{c0}$.^{28,29} This is often used to explain the two-step form of the resistive superconducting transition in high-temperature ceramics.³⁰ The J component of the superconducting response, coming into play at a lower temperature, causes the total resistance of the material to vanish. In our case the fraction of Josephson junctions is apparently small. Correspondingly, the J component is also small.

One other limiting case is known. Intragranular gaps can still admit direct tunneling, but their normal resistance can be so high that fluctuations suppress the coherent Josephson current.³¹ If the current between granules is controlled by single-particle tunneling, then a decrease of the temperature and opening of the superconducting gap at the Fermi level results in exponential growth of the resistance.⁴⁻⁶ This is also a component of the superconducting response, but it is associated not with the superconducting current but rather with the incoherent quasi-particle current.

3.2. Dynamic susceptibility

Figure 5 displays the normalized temperature dependence of the dynamic susceptibility $\chi(T)$ in different states of the sample. Unity on the ordinate corresponds to complete expulsion of magnetic flux from the volume occupied by the sample.

In a spatially nonuniform medium the dynamic-susceptibility signal consists of the Meissner effect proper in superconducting granules and screening of normal regions due to Josephson currents between granules. These contributions can be separated by changing the amplitude of the measuring ac current. For extremely low amplitudes the curve $\chi(T)$ contains both contributions (upper limiting curve in the terminology of Ref. 32). An increase of the amplitude results in breaking of Josephson bonds and a decrease of the signal $\chi(T)$. For sufficiently large ampli-

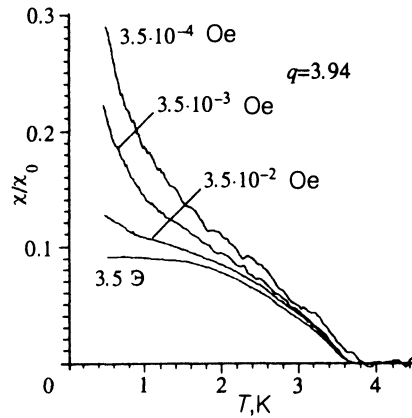


FIG. 6. Normalized dynamic-susceptibility signal for different amplitudes of the ac field.

tudes the signal no longer depends on the amplitude. The lower limiting curve,³² reflecting only the Meissner part of the susceptibility, is obtained.

The curve $q=0$ in Fig. 5 is the upper limiting curve. Increasing the field amplitude H_{ac} did not decrease the signal, either because the Josephson links were quite strong and the amplitudes available to us were insufficient to break them or because the superconducting state in the initial metastable metal phase was, in general, uniform. Amplitude dependence of the curve $\chi(T)$ appeared in subsequent intermediate states of the sample with $q > 0$ (Fig. 6). As q increased, the interval in which amplitude dependence was observed shifted toward lower amplitudes, and for large q we recorded, in general, only the lower limiting curve. All curves in Fig. 5, except for the $q=0$ curve, can be regarded as lower bounds.

Even the fact that the curve $\chi(T)$ contains only the Meissner part of the susceptibility makes it impossible to estimate the fraction of the superconducting phase in the sample as long as the size r of the superconducting particles relative to the penetration depth λ of a magnetic field in the superconductor is unknown. If the magnetic moment \mathfrak{M} of superconducting particles with size $r \gg \lambda$ is taken as unity, when penetration of the field can be neglected, then for particles of the same shape in the opposite limiting case

$$r \ll \lambda \quad (3)$$

we have

$$\mathfrak{M} = \gamma(r/\lambda)^2, \quad (4)$$

where the coefficient γ depends on the shape of the particles.³³ For a sphere of radius r we have $\gamma = \gamma_{sph} = 1/15$, for a cylinder of radius r we have $\gamma = \gamma_{cyl} = 1/8$, for a slab of thickness of $2r$ in a parallel field we have $\gamma = \gamma_{pl} = 1/3$, and so on. For this reason, the superconducting response in the dynamic susceptibility depends on the dispersity of the medium. For a fraction η of the superconducting volume the response is

$$\chi/\chi_0 = \eta \quad (5)$$

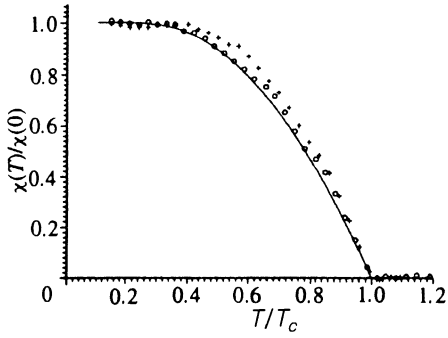


FIG. 7. Comparison of the temperature dependence of the dynamic-susceptibility signal in two high-resistance states of the sample with the theoretical curve constructed in the dirty London limit of the BCS theory with no free parameters: $q=4.8$ (\circ), 5.0 ($+$).

for the coarsely dispersed phase, when the size of the superconducting region satisfies $r \gg \lambda$, and

$$\chi/\chi_0 = \eta\gamma(r/\lambda)^2 \quad (6)$$

for the finely dispersed superconducting phase having characteristic size $r < \lambda$. Here χ_0 is the signal obtained when the magnetic flux is completely expelled from the volume of the sample.

The fine dispersion of the superconducting phase makes it possible to explain the existence of the temperature dependence $\chi(T)$ in states with large values of q . It is well known that λ is temperature-dependent, varying from λ_0 at low temperatures to infinity at $T = T_c$. If $r < \lambda_0$, then the relation (3) and therefore, the relation (6) hold in the entire temperature interval $0 < T < T_c$. Then the experimentally measured function F of $t = T/T_c$

$$\chi(T)/\chi(0) = [\lambda(T)/\lambda(0)]^{-2} \quad (7)$$

is determined only by the temperature dependence $\lambda(T)$ and does not depend on either the size or shape of the particles or on the spread of these parameters or the particle concentration.^{33,34}

In Fig. 7 such normalized temperatures $\chi(T)$ for the states $q=4.8$ and $q=5$ are compared to the theoretical curve calculated in the BCS model in the dirty London limit

$$l \ll \xi \ll \lambda, \quad (8)$$

where l is the mean free path length. This comparison proves that it is the fine dispersion of the superconducting phase that determines the temperature dependence $\chi(T)$ observed in these high resistance states.

4. DISCUSSION

4.1. Effective-medium approximation

We now construct a model in which all three components of the superconducting response are present simultaneously: decrease of the resistance due to the presence of superconducting granules and due to Josephson currents

and growth of the resistance due to freezing-out of the single-particle tunneling current between superconducting granules.

We employ the effective-medium approximation,³⁵ where the average values of the conductivity σ_m are obtained by averaging the conductivities σ_{kl} of the bonds in the lattice from the equation

$$\frac{2}{z} = \left\langle \frac{\sigma_{kl}}{\sigma_{kl} + \sigma_m(z/2 - 1)} \right\rangle; \quad (9)$$

here z is the number of bonds per lattice site and the brackets indicate averaging. Consider a simple cubic lattice ($z = 6$) consisting of metal grains, and let a fraction p of the bonds between the grains have tunneling conductivity $\sigma_{kl} = \sigma_{\text{tun}}$ and the remaining $1-p$ fraction have hopping conductivity $\sigma_{kl} = \sigma_{\text{hop}}$. Assume that σ_{hop} is unaffected by either the superconducting transition or a magnetic field, but σ_{hop} has an activation character and depends on the temperature, for example, according to Mott's law: $\sigma \propto \exp[-(T_0/T)^{1/4}]$. The conductivities σ_{tun} do not depend on T above T_c , but they freeze out below T_c according to the law

$$\sigma_{\text{tun}} = \sigma_t \exp(-\Delta/T). \quad (10)$$

A magnetic field, destroying superconductivity, restores them up to the value $\sigma_t = \sigma_{\text{tun}}(T_c)$. Two functions are measured: the conductivity $\sigma_{m0}(T)$ with no field and the conductivity $\sigma_{mH}(T)$ in a field with the superconducting interaction destroyed.

The fact that σ_{m0} decreases with temperature more slowly than according to the law (10) implies that there is an infinite cluster of bonds σ_{hop} , i.e., that $p < 2/3$. Suppose that in a magnetic field, when $\sigma_{\text{tun}}(T) \approx \sigma_{\text{tun}}(T_c) \equiv \sigma_t$, the conductivities σ_{hop} and σ_{tun} are comparable and both types of bonds must be taken into account in Eq. (9). Then at temperatures $T \ll T_c$ the inequality $\sigma_{\text{tun}} \ll \sigma_{\text{hop}}$ obviously holds and we can set $\sigma_{\text{tun}}(H=0) = 0$.

At some temperature $T \ll T_c$ we obtain from Eq. (9)

$$2\sigma_{mH}^2 - \sigma_{mH}[(3p-1)\sigma_t + (2-3p)\sigma_{\text{hop}}] - \sigma_t\sigma_{\text{hop}} = 0, \quad (11)$$

$$\sigma_{\text{hop}} = \frac{2}{2-3p} \sigma_{m0}.$$

Hence we obtain a simple relation between the dimensionless quantities

$$\alpha(T) = \sigma_t/\sigma_{\text{hop}}(T) \quad \text{and} \quad u(T) = \sigma_{mH}/\sigma_{m0}, \quad (12)$$

namely

$$\alpha = (2-3p)^2 \frac{u(u-1)}{2 + (2-3p)(3p-1)u}. \quad (13)$$

Figure 8 displays three curves $\alpha(p)$ with different values of u . Two of these curves correspond to values of u demonstrated in Fig. 3. For the state $q=4.7$ the value $u=1.5$ is obtained for $T=0.5$ K and $u=1.2$ is obtained for $T=0.75$. The curves $\alpha(T)$ in Fig. 8 have vertical asymptotes: If the concentration p is too low, then even for very large α the required increase of the average conductivity cannot be obtained by activating the bonds σ_t . The dashed

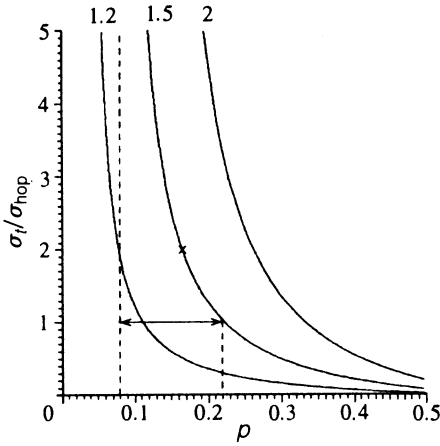


FIG. 8. $a(p) = \sigma_i/\sigma_{\text{hop}}$ [Eq. (13)] for $u = 1.2, 1.5$, and 2.0 . The vertical dashed line is the asymptote for the curve $u = 1.5$ and the arrow indicates the values of p for which $a > 1$ on this curve.

line is the asymptote of the curve $u = 1.5$. It follows from this asymptote that in the state $q = 4.7$ the relative concentration of tunnel bonds $p > 0.08$.

The relation (13) can in principle be compared to experiment, since p does not depend on T and the temperature dependences $\alpha(T)$ and $u(T)$ are measured experimentally. As the temperature increases we move in the (p, α) plane in Fig. 8 downward along the vertical to smaller values of u and, therefore, smaller values of α , i.e., larger values of σ_{hop} . The specific form of the function $\sigma_{\text{hop}}(T)$ depends on the value of p , which can be estimated from the expected values of α . If it is assumed that the tunneling gaps differ from the hopping gaps mainly by the width d

$$d_{\text{tun}} < d_{\text{hop}}$$

then it immediately follows hence that $\alpha > 1$. This limits the interval of possible values of p . In Fig. 8 this interval, determined with the help of the $u = 1.5$ curve, is marked with an arrow.

The maximum in weak fields can also be described by making the model slightly more complicated. Suppose that in zero field j of the p tunneling gaps become Josephson gaps. The first of the equations (11) remains unchanged. In writing the second equation we take into account the fact that the conductivity of the bonds in zero magnetic field is zero with probability $p - j$, infinity with probability j , and σ_{hop} with probability $(1 - p)$. For definiteness, we take the value $p = 0.82$, falling approximately at the center of the distinguished interval and corresponding to $\alpha = 2$ on the $u = 1.5$ curve. The observed 2% decrease of u (relative height of the maximum in the inset in Fig. 3) is obtained by introducing only $j/p \approx 2.5\%$ Josephson bonds.

Thus the upper curve in Fig. 3 can be described in this model with the parameters $\alpha = 2$, $p = 0.18$, and $j = 0.004$. Then as the temperature increases up to 0.75 K, since p and j are assumed to be constants, α must drop to 0.5, which corresponds to quadrupling of the conductivity σ_{hop} . Indeed, the conductivity of the sample at $H = 0$ in-

creases by only a factor of 1.7 (see Fig. 1d). This discrepancy characterizes the measure in which the model is suitable for describing our experiment.

The observed discrepancies should not be viewed as disappointing. The model employed is too rough in order to describe correctly the temperature dependences. The assumption that all bonds are divided into only two groups, without any dispersion and with identical temperature dependences within groups, is obviously an oversimplification of the real situation. However, this model demonstrates the main point: The superconducting response of a granular metal can indeed contain three components in the ratios which are observed experimentally.

4.2. Estimates of the characteristic lengths

The theory of superconductivity contains two parameters with the dimension of length: the penetration depth λ of a magnetic field and the coherence length ξ . In type-II superconductors they are related with the characteristic values of the magnetic field by the equations

$$\begin{aligned} H_{c1}(T) &= [\Phi_0/4\pi\lambda^2(T)] \ln \kappa, & H_{c2}(T) \\ &= \Phi_0/2\pi\xi^2(T), & \Phi_0 = \pi c\hbar/e, \end{aligned} \quad (14)$$

where κ is the Ginzburg-Landau parameter, and it is assumed here that $\kappa \ll 1$. In the dirty limit $\xi \gg l$ the quantity ξ in Eq. (14) must be replaced by an effective coherence length $\xi' = (\xi l)^{1/2}$.

We consider first measurements of H_{c2} and the values of ξ estimated from them. The right-hand scale, constructed with the help of Eq. (14), in Fig. 2 determines the scale of the correlation length ξ' : For $T < T_c$ the correlation length satisfies $\xi' \approx 100\text{--}200 \text{ \AA}$. This scale is the basis for all subsequent comparisons.

We determined the field H_{c2} according to the appearance of the superconducting response on the high-field side of the curves $R(H)$. In classical type-II superconductors this method for determining the field H_{c2} is facilitated by pinning: Pinning of flux lines prevents losses due to motion of the flux lines in a field $H < H_{c2}$ and makes the change in resistance in the field H_{c2} sharper. In the absence of pinning the resistive state is determined by flux line motion and is extended to the field H_{c1} . The response of the dynamic susceptibility χ to a magnetic field and the role of pinning are, to some degree, opposites. On the curves of the dynamic susceptibility $\chi(H)$ the signal should decrease in the field H_{c1} , because for $H > H_{c1}$ the flux lines penetrate into the superconductor and the magnetic moment drops sharply. But, in order that the penetration of flux lines be reflected in the dynamic susceptibility the flux-line lattice must fluctuate in time with the external field. Pinning, by fixing the position of the flux lines, seemingly decouples the external alternating field from the internal constant field. For this reason, due to pinning the field H_{c1} is not very sharply manifested in the curves of the dynamic susceptibility and a strong signal can be observed right up to the field H_{c2} .

As shown above, in states with large q we are dealing with small superconducting regions. In a finely dispersed

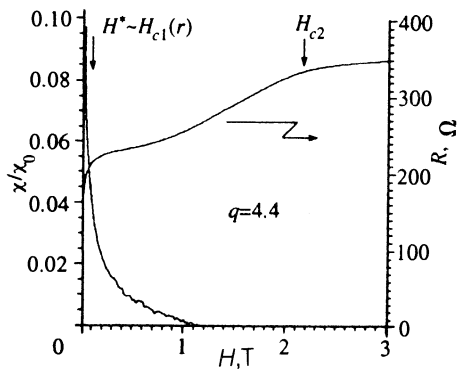


FIG. 9. Comparison of the field dependence of the resistance and susceptibility in the state $q=4.4$. The vertical arrows mark the field H^* (see text, Sec. 4.2) and H_{c2} .

medium the effect of pinning on the dynamic-susceptibility signal decreases, since the number of flux lines in each particle is small. For this reason the dynamic-susceptibility signal decreases near the field H_{c1} , i.e., in a much weaker field than the field in which the superconducting response completely vanishes on the curve $R(H)$ (see Fig. 9).

We now introduce the characteristic field H^* in which the signal $\chi(H)$ drops by a factor of 2. In Fig. 10 this field is displayed as a function of q . It is well known that fields larger than H_{c1} penetrate into small superconducting particles. For example, for a film of thickness $2r$ in a parallel field³⁶

$$H_{c1}(r) = (\Phi_0/2\pi r^2) \ln(2r/\xi), \quad \xi \ll r \ll \lambda. \quad (15)$$

It is this effect that apparently explains the dependence $H^*(q)$.

In all equations (14) and (15) the characteristic field is inversely proportional to the squared characteristic length. Neglecting logarithmic factors, in making estimates we always assumed that the coefficient of proportionality is $\Phi_0/2\pi$. It is this coefficient that was used to construct the right-hand scale in Fig. 10. The existence of the dependence $H^*(q)$ for $q > 4$ is itself natural and confirms the previously obtained inequality (3). But the estimate $\lambda \approx 1300 \text{ \AA}$, following from this plot, should not be taken

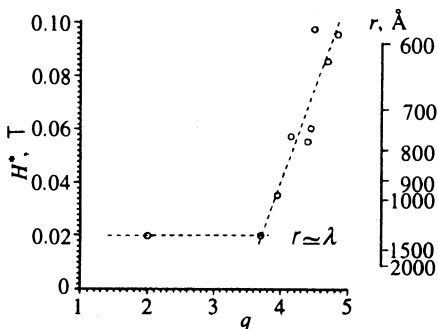


FIG. 10. H^* as a function of the parameter q .

too seriously, not only because we neglected logarithmic factors in Eqs. (14) and (15), but also because of the arbitrariness in defining H^* .

As one can see from Fig. 9, the field $H_{c1}(r)$ is of the same order of magnitude as the field H_J , in which the J component of the superconducting response is destroyed. For a flat contact of width $2r$ with a field in the plane of the contact the field H_J is

$$H_J = \Phi_0/4r\lambda. \quad (16)$$

Comparing Eq. (16) to Eq. (14) shows that the equality of $H_{c1}(r)$ and H_J indicates only that $r \approx \lambda$.

Thus comparing Figs. 2 and 10 shows that in high-resistance states

$$r \approx (3-5)\xi', \quad \text{i.e., } r > \xi'. \quad (17)$$

The limit of a "quasiuniform medium" $r < \xi'$ is close, but it is apparently still not reached in this material.

5. CONCLUSIONS

Thus, the effective-medium approximation and analysis of the effective lengths show that superconducting response evolution observed in Cd-Sb can be described in terms of the granular-superconductor model. This, however, does not resolve all questions.

The temperature dependence of the conductivity of this alloy near the metal-insulator transition is described very well by the temperature dependence¹⁸⁻¹⁹

$$\sigma - \sigma(0) \propto T^{1/3}, \quad (18)$$

in accordance with the theory constructed for a quasiuniform medium.^{37,38} One of the following three conclusions can logically be drawn from this.

1. It is possible that granular metal also has a critical region near the metal-insulator transition with temperature dependence of the type (18). In the insulator region the temperature dependence is similar in granular and quasiuniform media.^{11,14-16} In the metal region $\sigma(T)$ can also have corrections similar to the quantum corrections in metal.⁶ The behavior of the transport properties of granular metal in the critical region has not been studied, either theoretically or experimentally.

2. It can happen that our material is structurally quasiuniform and behaves correspondingly in the normal state, but that the superconducting transition itself stimulates the appearance of nonuniformity at the electronic level. According to Ref. 39, if the spatial fluctuations of the electronic characteristics are strong enough, the superconducting order parameter is not self-averaged and superconductivity becomes nonuniform and the superconducting regions arise at first in the form of separate drops. Phase separation at the electronic level in a superconducting transition was also discussed in Ref. 40. There is still no experimental evidence for such a scenario.

3. Finally, it can happen that the superconducting response of a quasiuniform material near the metal-insulator transition is similar, under certain conditions, to the superconducting response of granular metal. Then the *a priori*

assumption that we are dealing with granular metal made in the preceding section, could lead to incorrect conclusions.

From this standpoint Ref. 41, where giant negative magnetoresistance in granular Al was observed, is very interesting. This effect is very similar in magnitude and character to the effect observed in GaSb.⁶ In terms of the present paper this is the J component of the superconducting response. The significant difference between the effects in granular Al (Ref. 41) and in metastable GaSb (Ref. 6) is observed in the temperature dependence of the quantity

$$\Delta R = R(0) - R(H).$$

In Al the quantity ΔR does not vanish at the superconducting transition temperature T_c in finely dispersed Al (in this material—about $1.5 \text{ K}^{1,2}$), but rather it decreases continuously with increasing T right down to 4 K. We contrast this to the fact that according to all estimates^{1,2} the inequality $r < \xi'$ opposite to (17) was satisfied in the material employed.

Thus none of the three variants can be excluded. The problem of the superconducting response in high-resistance materials cannot be regarded as closed.

We thank E. G. Ponyatovskii for his interest in this work. This research was performed as part of the projects 93-02-2794 and 93-02-3271 of the Russian Foundation for Fundamental Research.

- ¹W. L. McLean, M. Kunchur, P. Lindenfeld, and Y. Z. Zhang, *Physica B* **152**, 230 (1988).
- ²M. Kunchur, Y. Z. Zhang, P. Lindenfeld *et al.*, *Phys. Rev. B* **36**, 4062 (1987).
- ³Y. Liu, D. B. Haviland, B. Nease, and A. M. Goldman, *Phys. Rev. B* **47**, 5931 (1993).
- ⁴C. J. Adkins, J. M. D. Thomas, and M. W. Young, *J. Phys. C* **13**, 3427 (1980).
- ⁵A. Gerber, *J. Phys.: Condens. Matter* **2**, 8161 (1990).
- ⁶V. F. Gantmakher, V. N. Zverev, V. M. Teplinskiĭ, G. É. Tsydynzhapov, and O. I. Barkalov, *Zh. Eksp. Teor. Fiz.* **104**, 3217 (1993) [*Sov. Phys. JETP* **77**, 513 (1993)].
- ⁷T. H. Lin, X. Y. Shao, M. K. Wu *et al.*, *Phys. Rev. B* **29**, 1493 (1984).
- ⁸Y. Tajuma and K. Yamada, *J. Phys. Soc. Jpn.* **69**, 495, 3307 (1984).
- ⁹B. Abeles, P. Sheng, M. D. Coutts, and Y. Arie, *Adv. Phys.* **24**, 406 (1975).
- ¹⁰P. Sheng, *Phil. Mag. B* **65**, 357 (1992).
- ¹¹M. Pollak and C. J. Adkins, *Phil. Mag. B* **65**, 855 (1992).
- ¹²E. Abrahams, P. W. Anderson, D. C. Licciardello, and T. V. Ramakrishnan, *Phys. Rev. Lett.* **42**, 673 (1979).

- ¹³P. A. Lee and T. V. Ramakrishnan, *Rev. Mod. Phys.* **57**, 287 (1985).
- ¹⁴M. Mostefa and G. Olivier, *Solid State Commun.* **70**, 489 (1989).
- ¹⁵O. Entin-Wohlman, Y. Gefen, and Y. Shapira, *J. Phys. C* **16**, 1161 (1983).
- ¹⁶R. Nemeth and B. Muhschlegel, *Z. Phys. B* **70**, 159 (1988).
- ¹⁷M. Tinkham, *Introduction to Superconductivity*, McGraw-Hill, New York, 1975.
- ¹⁸V. M. Teplinskiĭ, V. F. Gantmakher, and O. I. Barkalov, *Zh. Eksp. Teor. Fiz.* **101**, 1698 (1992) [*Sov. Phys. JETP* **74**, 905 (1992)].
- ¹⁹V. F. Gantmakher, V. N. Zverev, V. M. Teplinskiĭ, and O. I. Barkalov, *Zh. Eksp. Teor. Fiz.* **103**, 1460 (1993) [*Sov. Phys. JETP* **76**, 714 (1993)].
- ²⁰I. T. Belash, V. F. Degtyareva, E. G. Ponyatovskii, and V. I. Rashupkin, *Fiz. Tverd. Tela* **29**, 1788 (1987) [*Sov. Phys. Solid State* **29**, 1028 (1993)].
- ²¹O. I. Barkalov, I. T. Belash, and A. F. Gurov, *Phys. Status Solidi A* **115**, K19 (1989).
- ²²O. I. Barkalov, I. T. Belash, V. F. Gantmakher *et al.*, *JETP Lett.* **48**, 609 (1988).
- ²³E. G. Ponyatovsky and O. I. Barkalov, *Mater. Sci. Rep.* **8**, 147 (1992).
- ²⁴V. F. Gantmakher, S. E. Esipov, and V. M. Teplinskiĭ, *Zh. Eksp. Teor. Fiz.* **97**, 373 (1990) [*Sov. Phys. JETP* **70**, 211 (1990)].
- ²⁵V. E. Antonov, A. E. Arakelyan, O. I. Barkalov *et al.*, *J. Alloys Compounds* **194**, 279 (1993).
- ²⁶O. I. Barkalov, E. G. Ponyatovsky, and V. E. Antonov, *J. Non-Cryst. Solids* **156-158**, 544 (1993).
- ²⁷V. F. Gantmakher, V. N. Sverev, V. M. Teplinskiĭ, and O. I. Barkalov, *JETP Lett.* **56**, 309 (1992).
- ²⁸A. Raboutou, J. Rosenblatt, and P. Peyral, *Phys. Rev. Lett.* **45**, 1035 (1980).
- ²⁹C. Ebner and D. Stroud, *Phys. Rev. B* **28**, 5053 (1983).
- ³⁰A. Gerber, T. Grenet, M. Cyrot, and J. Beille, *Phys. Rev. B* **45**, 5099 (1992).
- ³¹C. M. Falco, W. H. Parker, S. E. Trullinger, and P. K. Hansma, *Phys. Rev. B* **10**, 1865 (1974).
- ³²V. F. Gantmakher, A. M. Neminsky, and D. V. Shovkun, *Physica C* **177**, 469 (1991).
- ³³D. Shoenberg, *Superconductivity*, Cambridge, 1952.
- ³⁴V. F. Gantmakher, N. I. Golovko, I. G. Naumenko *et al.*, *Physica C* **171**, 223 (1990).
- ³⁵S. Kirkpatrick, *Rev. Mod. Phys.* **45**, 574 (1973).
- ³⁶A. A. Abrikosov, *Zh. Eksp. Teor. Fiz.* **46**, 1464 (1964) [*Sov. Phys. JETP* **19**, 988 (1964)].
- ³⁷Y. Imry, *J. Appl. Phys.* **52**, 1817 (1981).
- ³⁸A. M. Finkel'shtein, *JETP Lett.* **37**, 517 (1983).
- ³⁹L. N. Bulaevskii, S. V. Panyukov, and M. V. Sadovskii, *Zh. Eksp. Teor. Fiz.* **92**, 672 (1987) [*Sov. Phys. JETP* **65**, 380 (1987)].
- ⁴⁰A. A. Gorbatshevich, Yu. V. Kopae, and I. V. Tokatly, *Zh. Eksp. Teor. Fiz.* **101**, 971 (1992) [*Sov. Phys. JETP* **74**, 521 (1992)].
- ⁴¹H. K. Lin, P. Lindenfeld, and W. L. McLean, *Phys. Rev. B* **30**, 4067 (1984).

Translated by M. E. Alferieff